ELECTRONIC SUPPORTING INFORMATION

Cascade Strategy for Triggered Radical Release by Magnetic Nanoparticles Grafted with Thermosensitive Alkoxyamine

Basile Bouvet,[a] Saad Sene,[a] Gautier Félix,[a] Jeffrey Havot,[b] Gerard Audran,[b] Sylvain Marque,*[b] Joulia Larionova*[a] and Yannick Guari[a]*

[a]ICGM, Univ. Montpellier, CNRS, ENSCM, CNRS Montpellier, France, E-mail: joulia.larionova@umontpellier.fr

[b]Aix Marseille Univ, CNRS, ICR, UMR 7273, Avenue Escadrille Normandie-Niemen, 13397 Marseille CEDEX 20, France, g.audran@univ-amu.fr, sylvain.marque@univ-amu.fr

Estimation of the number of alkoxyamines on the surface of the nanoparticles 3.

The number of ligands grafted on the surface of the nanoparticles was first estimated using SEM-EDS analysis. As the alkoxyamine ligand **2b** bears a phosphorous atom, a correlation between iron and alkoxyamine can be established from the ratio P/Fe:

$$Number\ of\ P\ per\ nanoparticle\ = \frac{\omega\frac{P}{Fe} \times N(Fe_{lattice})\ \times V_{NP}}{V_{lattice}}$$

with $\omega\frac{P}{Fe}$ is the P/Fe ratio obtained from SEM-EDX measurements, $N(Fe_{lattice})$ and $V_{lattice}$ are the number of Fe atoms (*i.e.* 24) and the volume of the lattice in the magnetite FCC lattice, respectively, V_{NP} and S_{NP} are the volume and surface of a nanoparticle, respectively.

The alkoxyamine concentration in a suspension of IONP@alkoxyamine can then be estimated using:

$$[Alkoxyamine] = \frac{m_{NP} \times\ Number\ of\ P\ per\ NP}{d_{NP} \times\ V_{NP}\ \times\ N_A\ \times\ V}$$

with N_A is the Avogadro number, d_{NP} is the density of the material (5.17 g.cm^{-3}), and V is the total volume of the suspension. The estimated number of phosphorus per nm^2 is equal to 1.95.

Quantification of radical's release by EPR analysis.

A suspension of IONP@alkoxyamine nanoparticles **3** (10^{-3} M) in *tert*-butylbenzene was submitted to the action of an ac magnetic field (≈ 20 mT at a frequency of 350 kHz). At each timepoint, 100 µL was withdrawn and cooled in an ice bath to stop the reaction. After magnetic separation, 50 µL of the supernatant was analysed by EPR.

A correlation between intensities measured by EPR and concentrations of alkoxyamines was performed using a calibration at three concentrations (10^{-4} M, 10^{-5} M, and 10^{-6} M) of alkoxyamine in *tert*-butylbenzene, in order to obtain an intensity value (I_{ref}) for a reference concentration (C_{ref}). Those solutions had been incubated at 120 °C overnight and measured by RPE. From each supernatant analysed during the kinetic study, the intensity of the first peak is measured, and the conversion rate in radicals was estimated using this following equation:

$$\frac{C}{C_0} = \frac{I \times C_{ref}}{C_0\ \times I_{ref}}$$

with C_0 = 1 mM is the initial concentration, and I is the intensity of the first peak measured by EPR at each timepoint. When plotted as a function of time, the kinetic constant k_d can be determined with the slope of the linear regression. The temperature at the surface of the nanoparticles can be estimated by using the Arrhenius law:

$$k_d = A \times exp(-E_a/RT) \text{ and}$$

$$T = \frac{-E_a}{R \cdot Ln(\frac{k_d}{A})}$$

where E_a is the activation energy, $A = 2.4 \cdot 10^{14}$ s^{-1} is the pre-exponential factor in the case of the alkoxyamine homolysis, R is the perfect gas constant and k_d is a homolysis constant.

Numerical resolution and fit of the homolysis/recombination law:

As mentioned in the main text, the couple of concentration equations is written as follows:

$$\frac{d[alkoxyamine]}{dt} = -k_d[alkoxyamine]$$

$$\frac{d[nitroxide]}{dt} = k_d[alkoxyamine] - k_1[nitroxide]$$

with:

$$k_d = A \times exp(-E_a/RT(t))$$

and:

$$T(t) = (T_{max} - T_0)(1 - exp(-t/\tau_T)) + T_0$$

As the k_d variable depends on the time, the differential equations do not admit an analytical solution. Then the solution of the equation was obtained by using a discretization of the differential equation:

$$[nitroxide](t + \Delta t) = [nitroxide](t) + \Delta t(k_d[alkoxyamine](t) - k_1[nitroxide](t))$$

$$[alkoxyamine](t + \Delta t) = [alkoxyamine](t) - \Delta t \cdot k_d[alkoxyamine](t)$$

Which can be rewritten as follows:

$$\frac{[nitroxide](t+\Delta t)}{C_0} = \frac{[nitroxide](t)}{C_0} + \Delta t\left(k_d \frac{[alkoxyamine](t)}{C_0} - k_1 \frac{[nitroxide](t)}{C_0}\right)$$

$$\frac{[alkoxyamine](t+\Delta t)}{C_0} = \frac{[alkoxyamine](t)}{C_0} - \Delta t \cdot k_d \frac{[alkoxyamine](t)}{C_0}$$

Fit of the magnetic nanoparticle assisted heating and SAR extraction:

The SAR (in $W\,g^{-1}$) is defined as follows:

$$SAR_{Fe} = \frac{P}{m_{Fe}} \quad or \quad SAR_{NP} = \frac{P}{m_{NP}} \tag{1}$$

With SAR_{Fe} and SAR_{NP} the SAR defined with the mass of Fe (m_{Fe}) or the mass of the magnetic nanoparticle (NP) (m_{NP}), respectively. P represents the power produced by the magnetic hyperthermia phenomenon. In this article, we will use m_{NP} as reference.

Usually, the SAR values are calculated in the adiabatic approximation (no energy exchange between the sample and the environment):

$$P = m_f c_f \cdot \frac{dT}{dt} \tag{2}$$

$$SAR_{NP} = \frac{m_f c_f}{m_{NP}} \cdot \frac{dT}{dt} \tag{3}$$

where m_f and c_f are the mass and the weighted heat capacity of the fluid, respectively.

If we want to take into account the possibility of energy exchange between the sample and the environment, we need to rewrite the equation (2). The Newton temperature equation law is a simple phenomenological model, which tends to reproduce the thermal evolution of such case. Equation (2) becomes:

$$m_f c_f \cdot \frac{dT}{dt} = P - h \cdot A \cdot (T - T_0) \tag{4}$$

with *h* is a phenomenological term for the energy transfer between the sample and the environment, *A* represents the area where the transfer occurs and T_0 is the temperature of the environment.

The solution of the differential equation (4) is:

$$T(t) = \frac{P}{hA} + T_0 - \frac{P}{hA} \cdot \exp\left(-\frac{hA}{m_f c_f} t\right) \tag{5}$$

However, in some case this phenomenological law cannot be sufficient. More generally, the energy transfer between the sample and the environment can be represented by an unknown function, which depends on T and T_0. We will define this function as $f(T,T_0)$. Then, equation (2) becomes:

$$m_f c_f \cdot \frac{dT}{dt} = P - f(T,T_0) \tag{6}$$

If we consider that T_0 is fixed and the difference between T and T_0 is small, then $f(T,T_0)$ has only one variable $f(T)$ and can be write using the Taylor series. For order 1 we have:

$$m_f c_f \cdot \frac{dT}{dt} = P - (T - T_0)\frac{\partial f(T_0)}{\partial T} \tag{7}$$

Equation (7) is in fact the Newton equation law, and admits an analytical solution.

If equation (7) is not sufficient to reproduce the experimental behavior, we can try to use the order 2 of the Taylor series of $f(T)$:

$$m_f c_f \cdot \frac{dT}{dt} = P - (T - T_0)\frac{\partial f(T_0)}{\partial T} - \frac{(T - T_0)^2}{2}\frac{\partial^2 f(T_0)}{\partial T^2} \tag{8}$$

This differential equation is more complex. We have chosen to solve this equation numerically, using the finite difference method:

$$T(t + \Delta t) = T(t) + \frac{\Delta t}{m_f c_f}\left(P - \left(T(t) - T_0\right) \cdot A - \left(T(t) - T_0\right)^2 \cdot B\right) \tag{9}$$

With, $A = \frac{\partial f(T_0)}{\partial T}$ and $B = \frac{1}{2}\frac{\partial^2 f(T_0)}{\partial T^2}$.

It is interesting to note that:

$$m_f c_f = \frac{m_{NP} \cdot c_{V,f}}{C_{NP}} \tag{10}$$

with m_{NP}, $c_{V,f}$ and C_{NP} are the mass of the nanoparticles, the volume heat capacity of the fluid and the concentration of nanoparticles, respectively.

Equations (7) and (8) were used to fit the experimental data shown on Figure S11. The extracted SAR_{NP} from equation (7) and (8) are equal to 259 ± 1 W/g and 420 ± 1 W/g, respectively. The value of 420 ± 1 W/g will be held since the equation (8) provides the best fit. The parameters used for these fits are $C_{NP} = 4$ mg mL^{-1} and $c_{V,f} = 1.538$ J.mL^{-1}.K^{-1}.

The ILP may be calculated as:

$$ILP = \frac{SAR}{f \cdot H^2} \tag{10}$$

COSMOL simulation:

Figure S12 shows the mapping of the magnetic field produced by the coils. COSMOL software with the magnetic extension was used to solve the Maxwell equations with infinite boundary conditions, for our specific geometry.

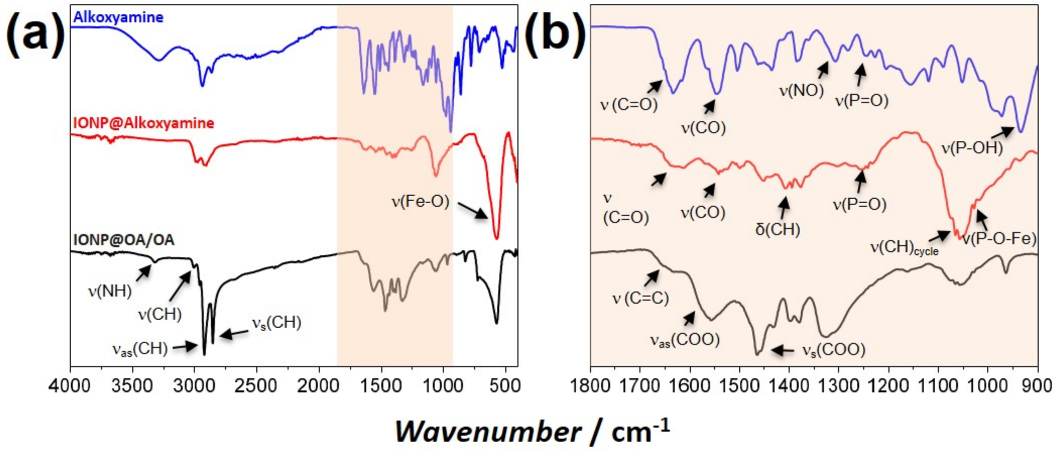

IONP@ OA/OA	Alkoxyamine	IONP@ Alkoxyamine	Assigments
3314	**-**	**-**	ν(N−H) NH_2
3001	**2989**	**-**	ν(C−H) CH_3
2921	**2909**	**2930**	ν_{as}(C−H) CH_2
2846	**-**	**2852**	ν_s(C−H) CH_2
1658	**-**	**-**	ν(C=C)
-	**1633**	**1633**	ν(C=O) amide
1559	**-**	**-**	ν_{as}(COO)
-	**1545**	**1542**	ν(C−O)
1465	**-**	**-**	ν_s(COO)
1380	**1380**	**1380**	δ(C−H) CH_2
-	**1307**	**1305**	ν(N−O)
-	**1247**	**1247**	ν(P=O)
-	**1053**	**1053**	ν(C−H)$_{cycle}$
-	**-**	**1027**	ν(P−O−Fe)
-	**935**	**-**	ν(P−OH)
564	**-**	**564**	ν(Fe−O)

Figures

Figure S1. IR spectra of IONP@OA/OL 1, IONP@alkoxyamine **3** and free alkoxyamine **2b** in: (a) the 4000–400 cm^{-1} window, and (b) the magnification in the range 1800–900 cm^{-1}; c) Table of the characteristic bands' assignment.

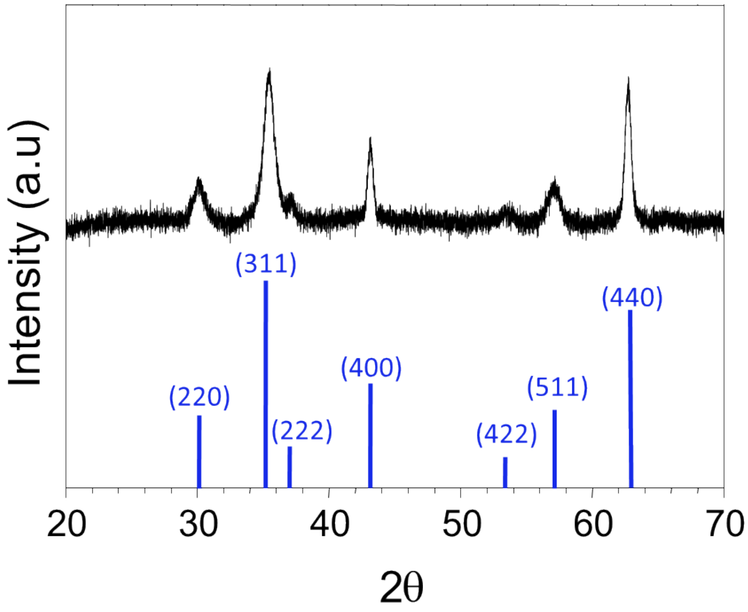

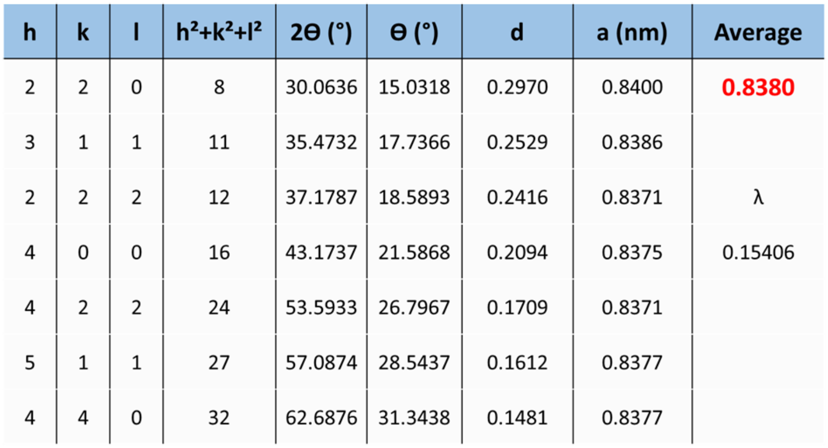

h	k	l	$h^2+k^2+l^2$	2θ (°)	θ (°)	d	a (nm)	Average
2	2	0	8	30.0636	15.0318	0.2970	0.8400	**0.8380**
3	1	1	11	35.4732	17.7366	0.2529	0.8386	
2	2	2	12	37.1787	18.5893	0.2416	0.8371	λ
4	0	0	16	43.1737	21.5868	0.2094	0.8375	0.15406
4	2	2	24	53.5933	26.7967	0.1709	0.8371	
5	1	1	27	57.0874	28.5437	0.1612	0.8377	
4	4	0	32	62.6876	31.3438	0.1481	0.8377	

a)

b)

Figure S2. a) XRD pattern of IONP@OA/OA **1** powder and reference diffraction peaks corresponding to Fe_3O_4; b) Table showing the calculation of the lattice constant of 8.38 Å.

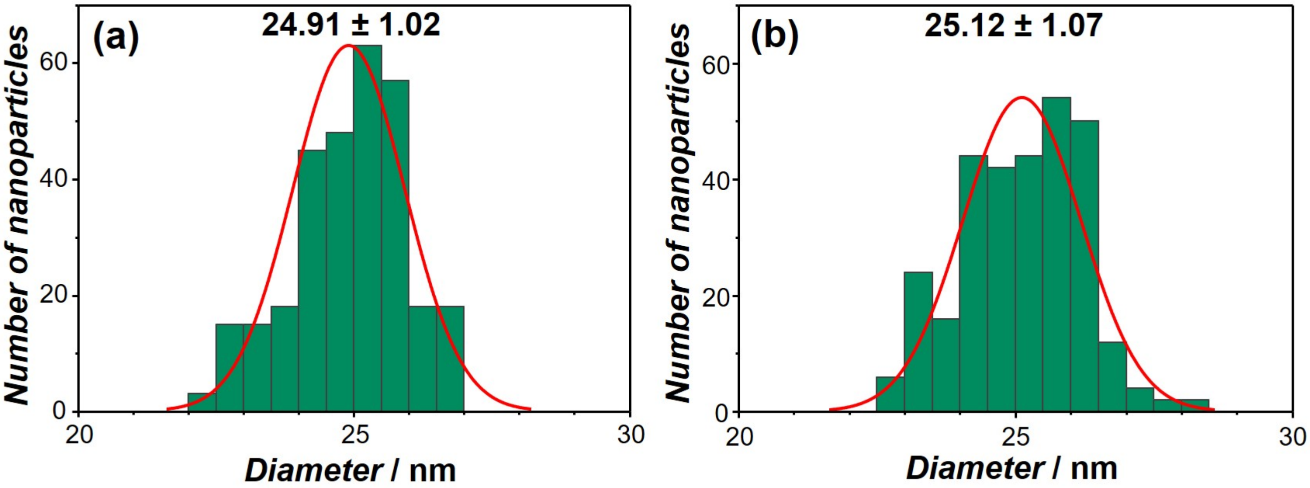

Figure S3. Histograms for the size distribution of (a) IONP@OA/OA **1** and (b) IONP@alkoxyamine **3** drawn from TEM images.

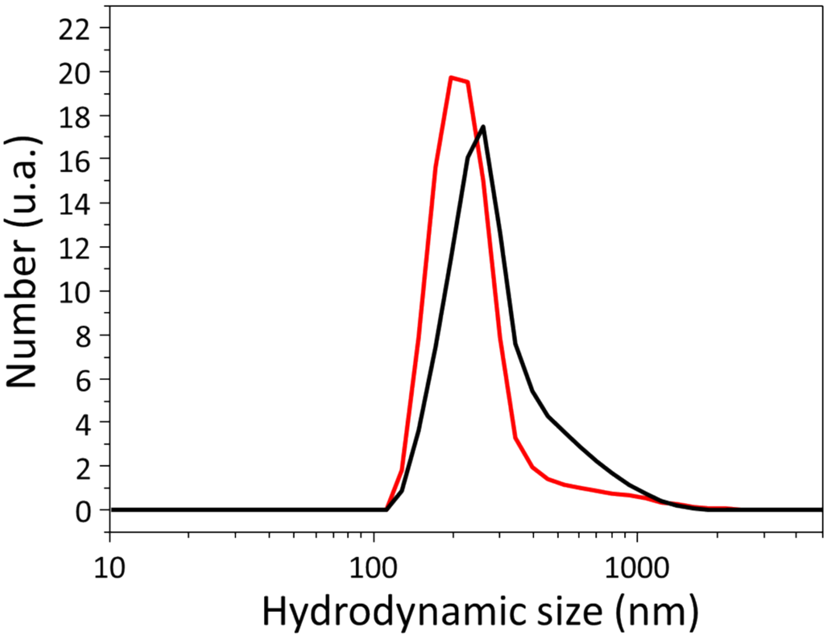

Figure S4. Hydrodynamic diameter distribution of IONP@OA/OA **1** (red) in cyclohexan and IONP@alkoxyamine **3** (black) in tert-butylbenzene, obtained using Dynamic Light Scattering (DLS).

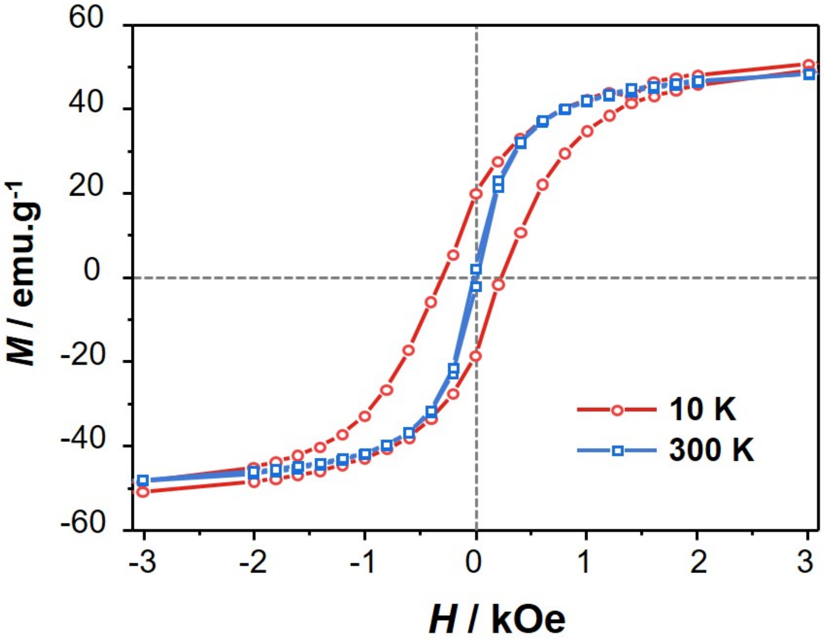

Figure S5. Hysteresis loop performed for **1** at 10 K (red circles) and 300 K (blue squares) shown between -3 and 3 kOe. The values of the saturation magnetization are equal to 69 and 62 emu.g^{-1} (at 5 T) at 10 and 300 K, respectively. The coercive field is 428 and 45 Oe at 10 and 300 K, respectively.

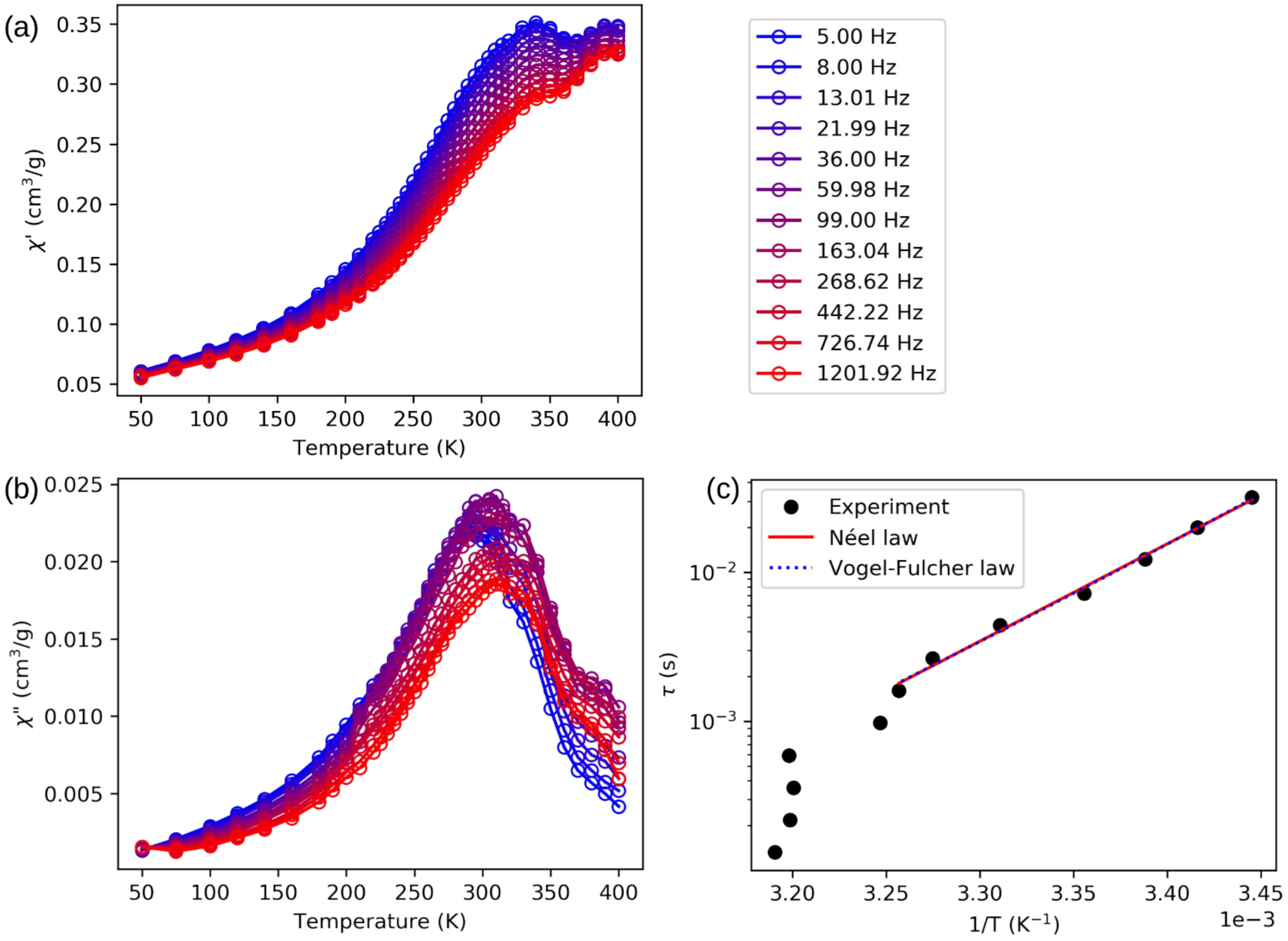

Figure S6. (a) In-phase and (b) out-of-phase ac magnetic susceptibility as a function of temperature at different frequencies for **3**. (c) Relaxation times, in a log scale, as a function of the inverse of temperature extracted from the frequency dependence of the out-of-phase component of the ac susceptibility (black circle) for **3**, and theoretical fit of relaxation times for the low frequency region with the Néel law (red line) and Vogel-Fulcher law (blue dashed line).

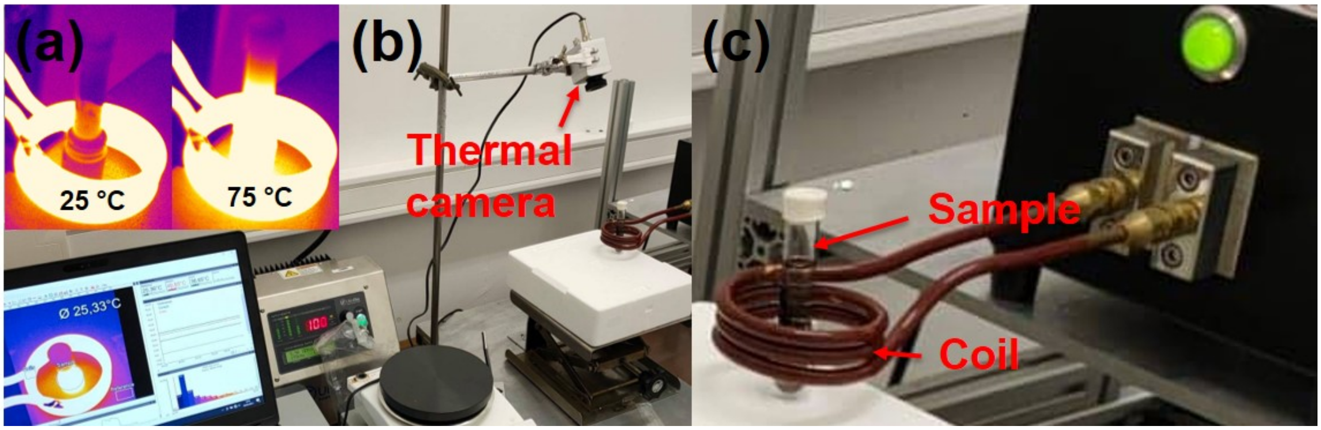

Figure S7. Photographs of the set-up during magnetic heating experiments of **3**: (a) Images of **3** obtained by thermal camera during magnetic heating; (b) magnetic nanoparticles assisted heating set-up and (c) the electromagnetic coil employed.

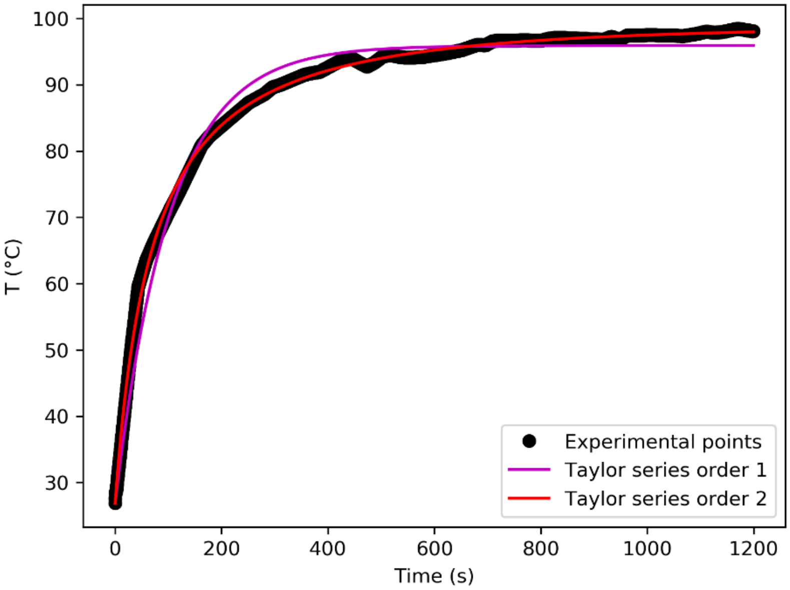

Figure S8. Magnetic nanoparticle-assisted heating curve (*T vs time*), with experimental points (black points) and the best fits using the first (eq. (7)) (magenta line) and the second order Taylor series model (eq. (8)) (red line).

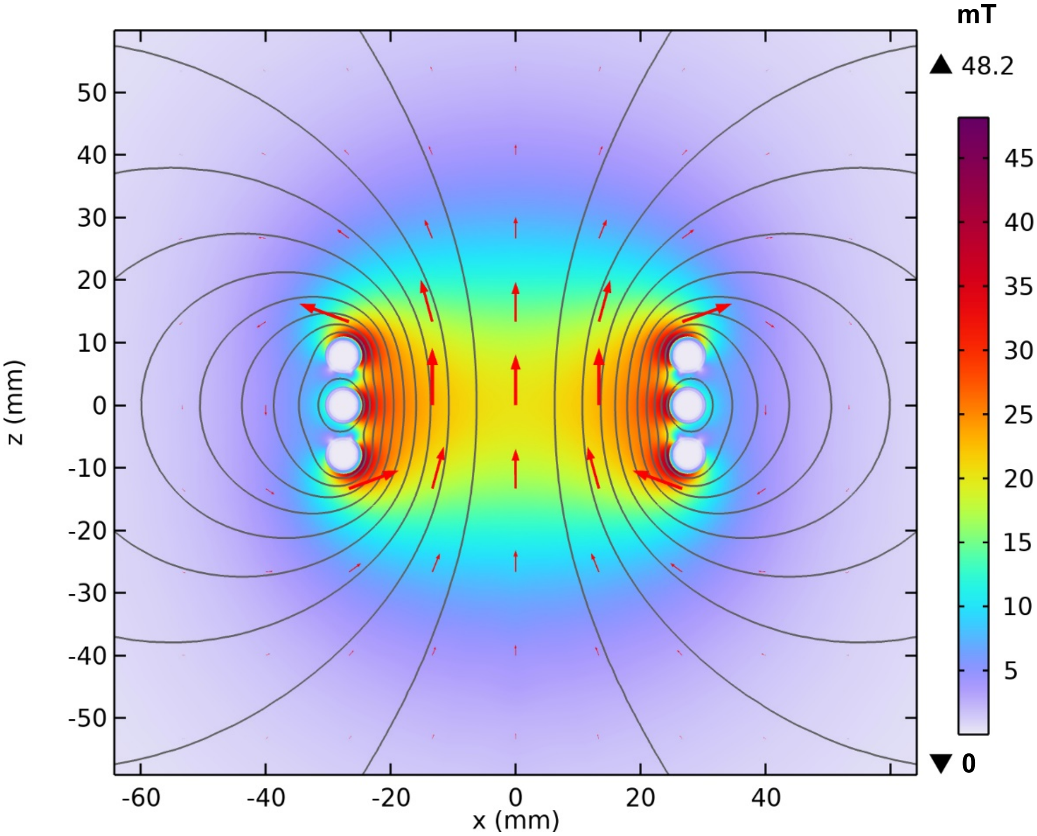

Figure S9. Mapping of the magnetic field intensity in mT with the magnetic field lines in black and the representation of the magnetic field direction by red arrows.

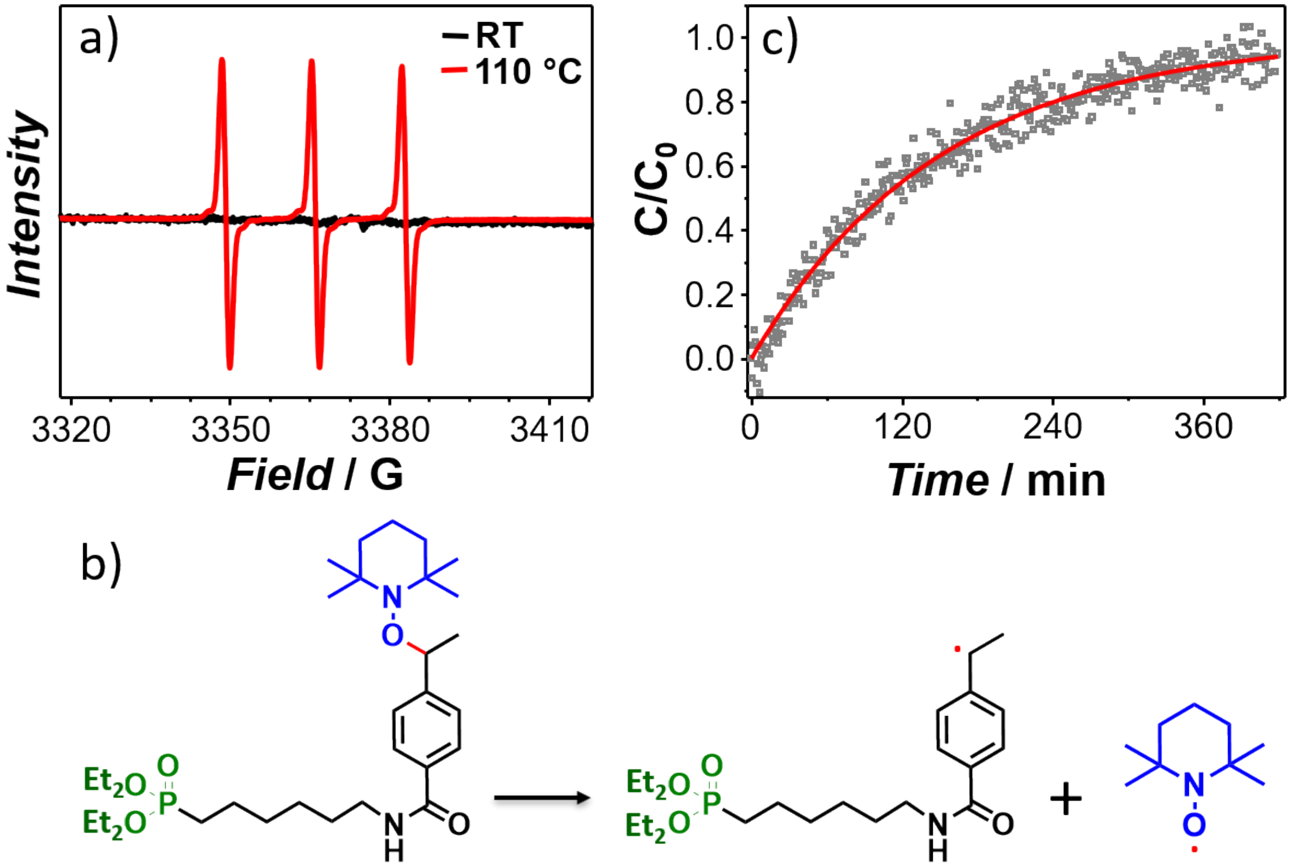

Figure S10. a) EPR spectra for the *tert*-butylbenzene solution of alkoxyamine **2a** (10^{-4} M) before (black) and after thermal heating to 115 °C during 5.5h (red); b) C/C_0 *vs.* time curve for alkoxyamine **2a** under heating; c) Schematic representation of the radical formation for alkoxyamine **2a** under thermal heating.

Note that the homolysis of **2b** investigated in water/n-PrOH (1/1) mixture as solvent (**2b** is not soluble in *tert*-butylbenzene) afforded $k_d = 1.1\ 10^{-4}$ at 90 °C and $E_a = 127.7$ kJ.mol^{-1}.

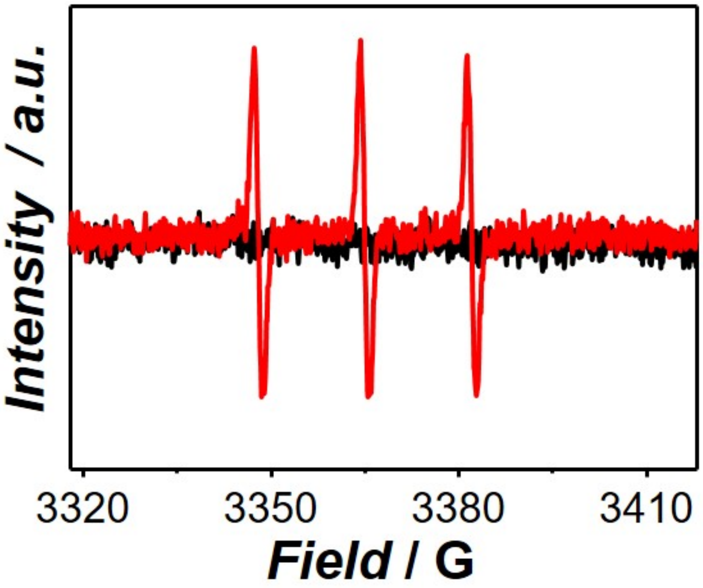

Figure S11. EPR spectrum of IONP@alkoxyamine **3** before (black) and after heating at 110 °C (red).

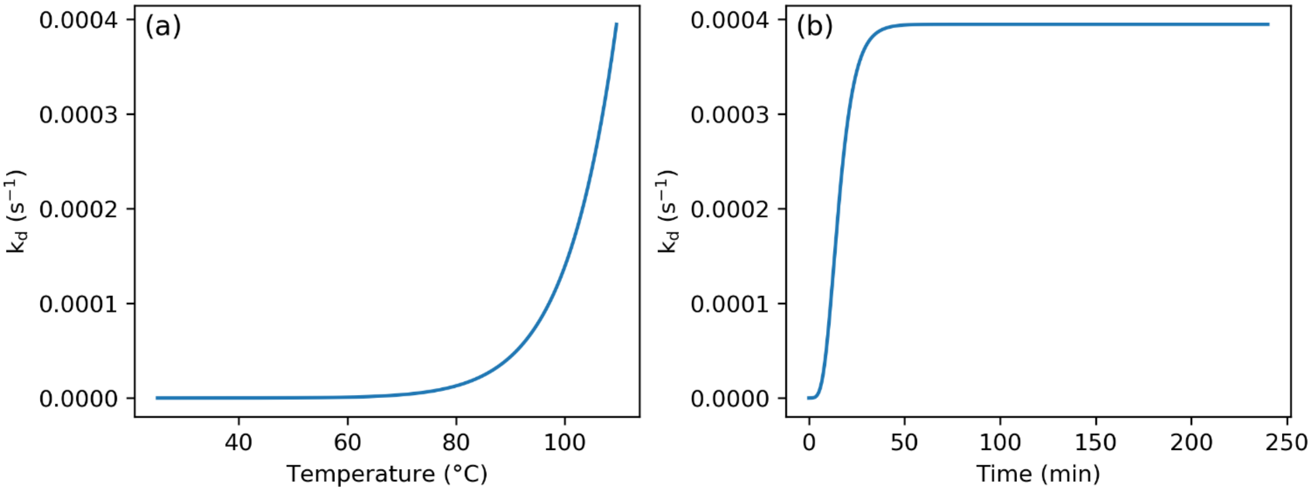

Figure S12. The k_d parameter as a function of temperature (a) and time (b) used in numerical simulations for **3**.

References

1 W. Su, S. Urgaonkar, J. G. Verkade, Organic Letters, **2004**, *6(9)*, 1421-1424

2 W. W. Yu, J. C. Falkner, C. T. Yavuz, V. L. Colvin, Chem. Commun. **2004**, *20*, 2306-2307